

waters for neodymium at molality 2.89,³⁰ but this number could change at the saturation molality of 3.93 where the electrolyte accommodates 5.1 less waters per neodymium.

The 6-hydrate nitrate series shows no abrupt changes in the $T\Delta S$ slope in Figure 3 that can be attributed to inner-sphere-bonding changes. However, data on all of the rare earths are needed to verify this conclusion. The large negative entropy change for each rare earth seems to be a result of moving nitrates inner sphere and removing inner-sphere water when the crystal is formed. Nitrate ion can penetrate the inner-sphere water structure and occupy two coordinate positions. The maximum number of inner-sphere nitrate positions is 10 for Ce(III),³¹ Ho(III),³² and Y(III)²⁰ when there is no inner-sphere water. In an analogous Sc(III) compound, only nine coordinate positions exist, with eight being bidentate and one monodentate.²⁰ The number of nitrates that will displace inner-sphere waters will depend not only on electrolyte and crystal compositions but also on cation size. Structural data are needed to determine whether the inner-sphere water in

Lu(NO₃)₃·5H₂O is one less than the other rare-earth cations.

We are unable at this time to make a complete assessment because of insufficient data. Solubility data and water activity data are needed for promethium chloride and nitrate electrolytes to establish the trend in crystallization behavior. Additional data are needed for the perchlorate series to establish $T\Delta S$ desolvation changes. Crystal structure determinations are needed for the perchlorate and nitrate series for evaluation of the desolvation mechanisms at saturation. Data for cerium and europium electrolytes are generally lacking.

In a following paper we calculate the energy requirements for desolvation of rare-earth perchlorates, chlorides, and nitrates from 0.1 *m* to saturation. We apply the second law for partial molal and integral changes.

Acknowledgment. The authors thank R. J. Bard, M. G. Bowman, and L. B. Asprey for discussions that helped considerably in writing this paper. We thank the U.S. Department of Energy, Office of Basic Energy Sciences, Division of Chemical Sciences, for support.

Registry No. [Pr₂Cl₂(H₂O)₁₄]Cl₄, 67573-46-0; [PrCl₂(H₂O)₆]₂Cl₂, 90432-19-2; [NdCl₂(H₂O)₆]₂Cl₂, 90432-20-5; [Pr(NO₃)₃(H₂O)₄]₂H₂O, 59964-37-3; Dy(ClO₄)₃·8H₂O, 90432-21-6; Lu(NO₃)₃·5H₂O, 34767-08-3.

(31) Al-Karaghoul, A.; Wood, J. S. *J. Chem. Soc., Dalton Trans.* 1973, 2318.

(32) Toogood, E.; Chieh, C. *Can. J. Chem.* 1975, 53, 831.

Contribution from the Departments of Chemistry, University of Michigan, Ann Arbor, Michigan 48109, and University of Chicago, Chicago, Illinois 60637

Electronic Switching of Ring Orientation in Cyclopentadienyl-Bridged Polymers

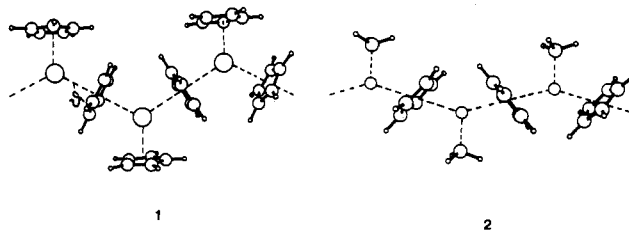
ENRICH CANADELL,*^{1a,b} ODILE EISENSTEIN,*^{1a,c} and TIMOTHY HUGHBANKS*^{1d}

Received December 1, 1983

The electronic and structural properties of cyclopentadienyl-bridged polymers (Cp₂Pb)_n and (CH₃ZnCp)_n are studied with a tight-binding method of band structure calculation. The orientation of the bridging cyclopentadienyl is related to the number of valence electrons at the metal center. In (Cp₂Pb)_n, the structure minimizes the antibonding interaction between the Pb and the bridging Cp occupied orbitals. In contrast, in (CH₃ZnCp)_n, which has two electrons less per metal center, the structure maximizes the bonding interaction between the empty Zn and the occupied Cp orbitals. The structural characteristics of (Cp₂Mn)_n are discussed. New types of polymers are suggested.

Since the discovery of ferrocene, dicyclopentadienyl complexes Cp₂M have come to form a large class of molecules.² Most of the complexes are monomeric in the gas phase and the solid state. Their structural and electronic properties have been extensively studied. The species Cp₂Pb³ polymerizes in the solid state as does a related species, CpZnCH₃.⁴ Both

of these systems are characterized as consisting of one-dimensional zigzag chains of metal atoms separated by bridging cyclopentadienyl ligands. Of particular interest is the orientation of the bridging cyclopentadienyl. In (Cp₂Pb)_n (1) the



bridging cyclopentadienyl is perpendicular to the vector joining adjacent Pb centers as if to coordinate each Pb in a η^2 fashion. An additional cyclopentadienyl ligand caps the metal in a η^5 fashion to complete the Pb coordination sphere. In CpZnCH₃ (2) the bridging cyclopentadienyl is inclined with respect to the Zn-Zn vector.⁴ In this orientation the cyclopentadienyl rings appear to become η^2 with respect to one metal center and η^3 with respect to the other.

A compound with obvious structural similarities to the above systems is Cp₂Mn,⁵ which polymerizes to form the structure

(1) (a) University of Michigan. (b) Present address: Department of Chemistry, University of Chicago. (c) Present address: Laboratoire de Chimie Théorique Batiment 490, Université de Paris-Sud, 91405 Orsay, France. (d) University of Chicago.

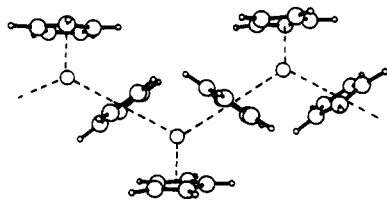
(2) For non transition metals: (a) Cp₂Pb: Almenningen, A.; Haaland, A.; Motzfeldt, T. *J. Organomet. Chem.* 1967, 7, 97. (b) Cp₂Ca: Zenger, R.; Stucky, G. *Ibid.* 1974, 80, 7. Diindenylmagnesium: Atwood, J. L.; Smith, K. D. *J. Am. Chem. Soc.* 1974, 96, 994. (c) (Me₂Cp)₂M (M = Ge, Sn, Pb): Bonny, A.; McMaster, A. D.; Stobart, S. R. *Inorg. Chem.* 1978, 17, 935. Atwood, J. L.; Hunter, W. E.; Cowley, A. H.; Jones, R. A.; Stewart, C. A. *J. Chem. Soc., Chem. Commun.* 1981, 925. Baxter, S. G.; Cowley, A. H.; Lasch, J. G.; Lattman, M.; Sharum, W. P.; Stewart, C. A. *J. Am. Chem. Soc.* 1982, 104, 4064. Almlöf, J.; Fernholt, L.; Faegri, K., Jr.; Haaland, A.; Schilling, B. E. R.; Seip, R.; Taubøl, K. *Acta Chem. Scand., Ser. A* 1983, A37, 131. (d) Jutzi, P.; Kohl, F.; Hofmann, P.; Krüger, C.; Tsay, Y.-H. *Chem. Ber.* 1980, 113, 757. (e) Cp₂As⁺: Baxter, S. G.; Cowley, A. H.; Mehrotra, S. K. *J. Am. Chem. Soc.* 1981, 103, 5572. (f) For the large subject of transition-metal metallocenes see, for instance, a review article by: Haaland, A. *Acc. Chem. Res.* 1979, 12, 415.

(3) Panattoni, C.; Bombieri, G.; Croatto, U. *Acta Crystallogr.* 1966, 21, 823.

(4) Aoyagi, T.; Shearer, H. M. M.; Wade, K.; Whitehead, G. *J. Organomet. Chem.* 1978, 146, C29. CpZnCH₃ monomeric: Haaland, A.; Samdal, S.; Seip, R. *Ibid.* 1978, 153, 187.

(5) Bündler, W.; Weiss, E. *Z. Naturforsch., B: Anorg. Chem., Org. Chem.* 1978, 33B, 1235.

3. As in CpZnCH_3 , the bridging cyclopentadienyl rings are



3

inclined to form a 65° angle with the Mn–Mn vector. This compound is also antiferromagnetic, a fact we will discuss briefly in light of its structure.

Why are the structures of these polymers as they are? Why do such different metal centers as Mn(II) and Zn(II) put the bridging cyclopentadienyl in a similar situation? Why does the Pb(II) induce a different structure? A better understanding of the structural properties of these polymeric chains is needed for an optimal design of further related compounds. Insofar as these systems have received little theoretical attention, in the present work we present band structures for these polymers. Focusing on a comparison of the Pb and Zn compounds discussed above, we show in which way the geometry of the bridging cyclopentadienyl is intimately related to the number of valence electrons at the metal center. The results may be used for predicting the structure of as yet unknown polymers.

Theoretical Procedure

The tight-binding (LCAO) method⁶ of band structure calculation based on the extended Hückel formalism was used. Given a set of basis atomic orbitals $\{\chi_\mu\}$ for the atoms of a unit cell, the set of the Bloch basis orbitals $\{b_\mu(\mathbf{k})\}$ are formed as

$$b_\mu(\mathbf{k}) = N^{-1/2} \sum_l e^{i\mathbf{k}\cdot\mathbf{R}_l} \chi_\mu(r - \mathbf{R}_l) \quad (1)$$

where \mathbf{k} is the wave vector, and $\mathbf{R}_l = l\mathbf{a}$ with \mathbf{a} being the primitive vector. With these Bloch basis orbitals the extended Hückel method leads to the eigenvalue equation

$$H(\mathbf{k}) C(\mathbf{k}) = S(\mathbf{k}) C(\mathbf{k}) e(\mathbf{k}) \quad (2)$$

where $H_{\mu\nu}(\mathbf{k}) = \langle b_\mu(\mathbf{k}) | H_{\text{eff}} | b_\nu(\mathbf{k}) \rangle$ and $S_{\mu\nu} = \langle b_\mu(\mathbf{k}) | b_\nu(\mathbf{k}) \rangle$. The solution of this eigenvalue problem results in LCAO crystal orbitals $\psi_n(\mathbf{k})$

$$\psi_n(\mathbf{k}) = \sum_\mu C_{n\mu}(\mathbf{k}) b_\mu(\mathbf{k}) \quad (3)$$

and eigenvalues $\epsilon_n(\mathbf{k})$. The band structure is then determined by performing the above calculation for various values of \mathbf{k} (usually within the first Brillouin zone; $-0.5\mathbf{K} < \mathbf{k} < 0.5\mathbf{K}$, where $\mathbf{K} = 2\pi/\mathbf{a}$). The parameters of the extended Hückel calculation are given in the Appendix. Experimental structural data were used for the polymers. A unit cell contains two LMCp units. Calculations were carried out to the nearest neighbor $l = -1, 0, +1$ in eq 1).

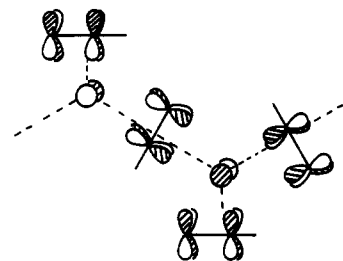
Results and Discussion

$(\text{Cp}_2\text{Pb})_n$. The total energy per unit cell is lower when the bridging cyclopentadienyl is perpendicular to the Pb–Pb direction ($\theta = 90^\circ$). A tilt of the cyclopentadienyl ($\theta = 80^\circ$) raises the energy by 0.8 eV/formula unit. To understand the reasons for this structural preference, we turn our attention to the band structure that is shown in Figure 1, parts a ($\theta = 90^\circ$) and b ($\theta = 80^\circ$). The symmetry group is isomorphic with C_{2v} at all \mathbf{k} points but at the zone edge ($\mathbf{k} = \pi/\mathbf{a}$). Accordingly, each band is labeled with C_{2v} symmetry symbols. A simplified symmetry label is also used for convenience. The screw axis which goes through the center of the bridging

cyclopentadienyl pairs up the a_1 bands with those of b_1 symmetry as well as those of a_2 and b_2 symmetry at the zone edge. The mirror plane containing the Pb centers can also be used for ascribing the symmetry of the bands at all \mathbf{k} points. Bands with labels a_1 and b_1 become S and a_2 and b_2 become A, where S and A label the bands with respect to this plane. Both sets of labels are used throughout this work. The C_{2v} labels are necessary to fully ascertain whether bands should cross or not; the simplified labels are often more easy to use.

In Figure 2, we show a solid-state Walsh diagram⁷ that illustrates the effect of the tilt of the bridging cyclopentadienyl. In this diagram the mean energy value of the bands is given as a function of θ . When the bands do not cross, such values are easily determined. When there are avoided crossings, as for the $1a_1$, $1b_1$, $2a_1$, and $2b_1$ bands, the calculation of the mean energy value is more ambiguous. The difficulty is avoided by adding the contributions of the bands in question in the Walsh diagram.

From the Walsh diagram (Figure 2), it appears that the mean energy values of the A bands are insensitive to the value of θ . In addition, the band structure indicates that the A bands are narrow. They are built from orbitals of cyclopentadienyl and Pb which overlap in a π fashion. As an example, the bottom of the $1a_2$ band ($\mathbf{k} = 0$) is shown in 4. Because of

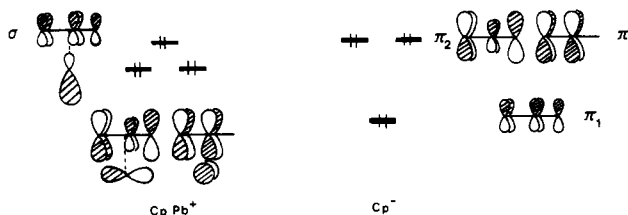


4

the large distance between the Pb centers and the bridging cyclopentadienyl, a π type overlap is small. Additionally, this overlap is only weakly θ dependent. Consequently, A bands will be neglected and the discussion will be focused on the S bands.

The Walsh diagram shows that the lower set of S bands ($1a_1 + 2b_1$) favor an angle θ of 80° while the higher S bands ($3a_1 + 3b_1$) strongly favor an angle θ of 90° . Turning our attention to the band structure, we see that the bottom of the $3a_1$ and $1a_1$ bands vary considerably with θ . The bottom of the $1a_1$ band ($\mathbf{k} = 0$) is stabilized at $\theta = 80^\circ$ while the bottom of the $3a_1$ band is considerably lower at $\theta = 90^\circ$. The other noticeable variation in the band structure comes from the $3b_1$ band, which is slightly more stable at $\theta = 90^\circ$. The other bands appear essentially at the same energy for both angles.

The relevant molecular orbitals of the two fragments CpPb^+ and Cp^- are shown in 5. The electronic characteristics of CpE



5

(6) Andre, J.-M. *J. Chem. Phys.* **1969**, *50*, 1536. Andre, J.-M. "Electronic Structure of Polymers and Molecular Crystals"; Andre, J.-M., Ladik, J., Eds.; Plenum Press: New York, 1974; p 1. Ladik, J. *Ibid.*, p 23.

(7) Walsh diagrams and correlation diagrams have been recently used for the analysis of the structure of solids: Wijeyesekera, S. D.; Hoffman, R. *Inorg. Chem.* **1983**, *22*, 3282. Kertesz, M.; Hoffmann, R., submitted for publication. Burdett, J. K.; Price, S. L. *Phys. Rev. B: Condens. Matter* **1982**, *25*, 5778. Canadell, E.; Eisenstein, O. *Inorg. Chem.* **1983**, *22*, 3856.

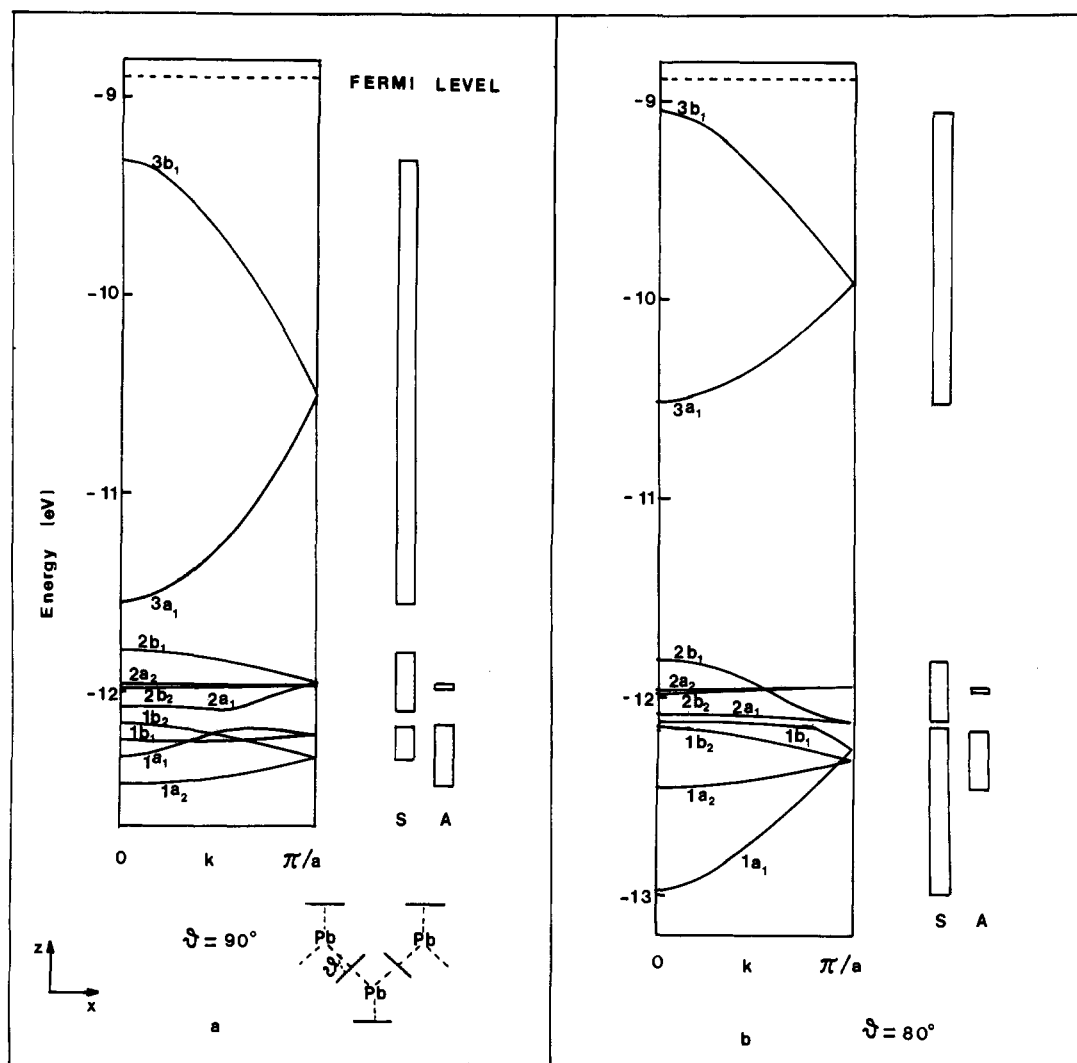
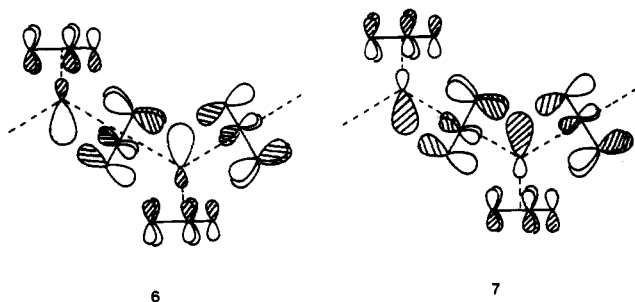


Figure 1. One-dimensional band structure for the $(\text{Cp}_2\text{Pb})_n$ chain at $\theta = 90^\circ$ (a) and at $\theta = 80^\circ$ (b). All bands shown are occupied.

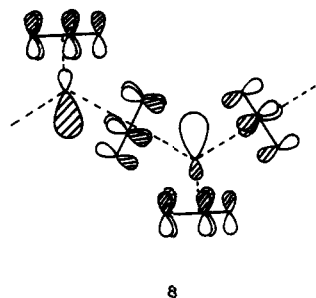
($\text{E} = \text{In}, \text{Tl}, \text{Sn}^+$)^{24,8,9} have been previously discussed and need no additional comments.

Each crystal orbital is made of linear combinations of fragment molecular orbitals of CpPb and Cp.¹⁰ Thus 6, which



represents the crystal orbital of $3a_1$ at $k = 0$, is made of the in-phase combination of the HOMO of CpPb, the σ lone pair on the Pb atom which mixes in an antibonding way with the lower energy π_2 cyclopentadienyl orbital. This antibonding interaction is large because σ and π_2 are close in energy. A decrease of the σ - π_2 overlap stabilizes 6. The minimum overlap is actually reached for $\theta = 90^\circ$. A tilt of the bridging cyclopentadienyl away from this position increases the overlap of π_2 with σ . A tilt of 10° doubles the σ - π_2 overlap (0.036, $\theta = 90^\circ$ vs. 0.073, $\theta = 80^\circ$). The crystal orbital of the $1a_1$ band at $k = 0$ is constructed from the in-phase combination of the π_2 cyclopentadienyl orbital, which mixes in a bonding way with the higher σ lone pair as shown in 7. An increase in the σ - π_2 overlap stabilizes 7. Consequently, 7 favors a tilt of the bridging cyclopentadienyl and is therefore more stable for $\theta = 80^\circ$ than for $\theta = 90^\circ$ (Figure 1).

The crystal orbital of the top of the $3b_1$ band ($k = 0$) is shown in 8. It results from the out-of-phase combination of



- (8) (a) Shibata, S.; Bartell, L. S.; Gavin, R. M., Jr. *J. Chem. Phys.* **1964**, *41*, 717. Pietro, W. J.; Blurock, E. S.; Hout, R. F.; Hehre, W. J.; DeFrees, D. J.; Stewart, R. F. *Inorg. Chem.* **1981**, *20*, 3650. Lin, C. S.; Tuck, D. G. *Can. J. Chem.* **1982**, *60*, 699. (b) Ewig, C. S.; Osman, R.; Van Wazer, J. R. *J. Am. Chem. Soc.* **1978**, *100*, 5017.
- (9) Nekrasov, Y. S.; Sizoi, V. F.; Zagorevskii, D. V.; Borisov, Y. A. *J. Organomet. Chem.* **1981**, *205*, 157.
- (10) The use of fragment molecular orbitals to analyze the electronic structure of solids finds fruitful application in the following examples: Hughbanks, T.; Hoffmann, R. *J. Am. Chem. Soc.* **1983**, *105*, 1150; *Inorg. Chem.* **1982**, *21*, 3578. Whangbo, M.-H.; Hoffmann, R. *J. Am. Chem. Soc.* **1978**, *100*, 6093. Whangbo, M.-H. "Extended Linear Chain Compounds"; Miller, J. S., Ed.; Plenum Press: New York, 1982; Vol. 2, p 127. Burdett, J. K. *J. Am. Chem. Soc.* **1980**, *102*, 450; "Structure and Bonding in Crystals"; O'Keeffe, M.; Navrotsky, A., Eds.; Academic Press: New York, 1981; Vol. 1, p 255.

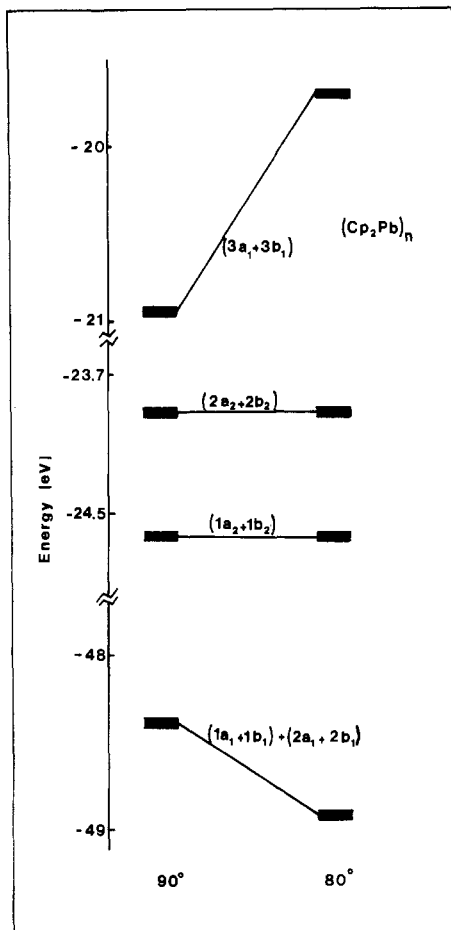


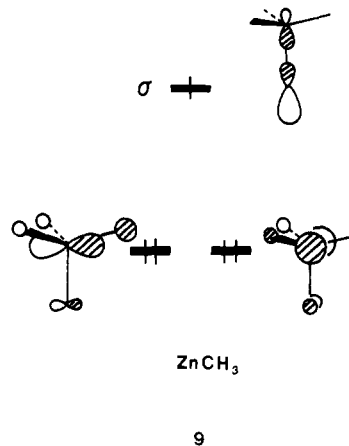
Figure 2. Solid-state Walsh diagram for the variation of θ from 90 to 80° in $(\text{Cp}_2\text{Pb})_n$.

the σ lone pairs, which is destabilized by the π_1 cyclopentadienyl orbital. The overlap between these two orbitals is large due to the absence of any nodal plane in π_1 , but the overlap at both angles is similar (0.137 at $\theta = 90^\circ$ vs. 0.142 at $\theta = 80^\circ$). This is merely because the Pb-centered hybrid is largely of s character, which contributes no angular dependence to overlap with the bridging cyclopentadienyl π_1 orbital. In addition, a large energy gap separates σ from π_1 . Consequently, the interaction $\sigma-\pi_1$, although it favors $\theta = 90^\circ$, is of lesser importance than the interaction $\sigma-\pi_2$ in imposing a given structure to the polymeric chain.

It therefore appears that the interaction of two orbitals, σ on CpPb and π_2 on the bridging cyclopentadienyl, determines the structure of the polymeric chain. In $(\text{Cp}_2\text{Pb})_n$ the bonding and the antibonding combinations of these orbitals are forming occupied bands. As the destabilization coming from the antibonding combination is larger than the stabilization coming from the bonding combination, the chain adopts a geometry that minimizes the overlap between these two fragment orbitals ($\theta = 90^\circ$).¹⁹

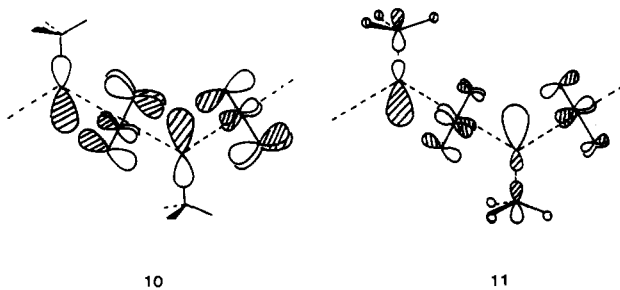
Finally, we should note that ideas often advanced about the 6s electrons being "inert" do not apply here. In fact, in our calculations we find the PbCp lone-pair fragment orbital (labeled " σ " in 5) to possess appreciable s character. Furthermore, if the 6s orbital was indeed inert, we would expect little or no geometrical preference. For these systems at least, the 6s orbitals are not "inert".

$(\text{CH}_3\text{ZnCp})_n$. The extension of the above analysis to the Zn polymer is immediate. ZnCH_3 is isolobal to CpPb^{2+} as shown in 9; i.e., the valence orbitals of the two fragments have similar nodal characteristics with the same number of electrons. Therefore, the replacement of CpPb by ZnCH_3 in the



polymer results in the removal of four electrons per unit cell (or two electrons per formula unit) from the highest bands $3a_1$ and $3b_1$. Occupancy of these two bands favors $\theta = 90^\circ$. When they are emptied of their electrons, the lower bands which are favoring the tilted position of the bridging cyclopentadienyl take over as is indeed found in the experimental result ($\theta = 65^\circ$).

This qualitative analysis is supported by the calculation. The total energy per formula unit is 0.95 eV lower for $\theta = 65^\circ$. The band structures are shown in Figure 3, parts a ($\theta = 90^\circ$) and b ($\theta = 65^\circ$). Symmetry labels similar to the ones in $(\text{Cp}_2\text{Pb})_n$ are used. The solid-state Walsh diagram is given in Figure 4. The mean energy value of the highest occupied S bands is stabilized by a tilt of the bridging cyclopentadienyl. The lower bands are virtually insensitive to the geometrical change. The crystal orbital at the bottom of the highest occupied band ($k = 0$) is shown in 10. Its analogy with 7 is



striking. It is made of the in-phase combination of the π_2 cyclopentadienyl orbital which mixes in a bonding way with the higher σ ZnCH_3 orbital. The antibonding counterpart of these two fragment orbitals appears in the empty bands with an additional strong stabilization produced by the empty π cyclopentadienyl orbital, 11 (bottom of the conduction band).

The four-electron destabilization $\sigma-\pi_2$, which is the dominating factor in $(\text{Cp}_2\text{Pb})_n$, is replaced by a two-electron stabilization $\sigma(\text{empty})-\pi_2(\text{occupied})$ in $(\text{CH}_3\text{ZnCp})_n$ with the concomitant reversal of the ring orientation.

$(\text{Cp}_2\text{Mn})_n$. Given the structural relationship between the $(\text{Cp}_2\text{Mn})_n$ polymer and the systems discussed heretofore, it is tempting to apply the above results to understand $(\text{Cp}_2\text{Mn})_n$. Magnetic susceptibility measurements have been done,¹¹ and the results indicate that Mn is reasonably formulated as a high-spin ion. Other structural evidence supports the idea of a high-spin ground state for this system; the η^5 capping cyclopentadienyl is quite far from the Mn center as compared with the corresponding distance in $\text{CpMn}(\text{CO})_3$ (in $(\text{Cp}_2\text{Mn})_n$ the average Mn-C distance is 2.42 Å, and in $\text{CpMn}(\text{CO})_3$ it

(11) König, E.; Desai, V. P.; Kanellakopulos, B.; Klenze, R. *Chem. Phys. Lett.* 1980, 54, 109.

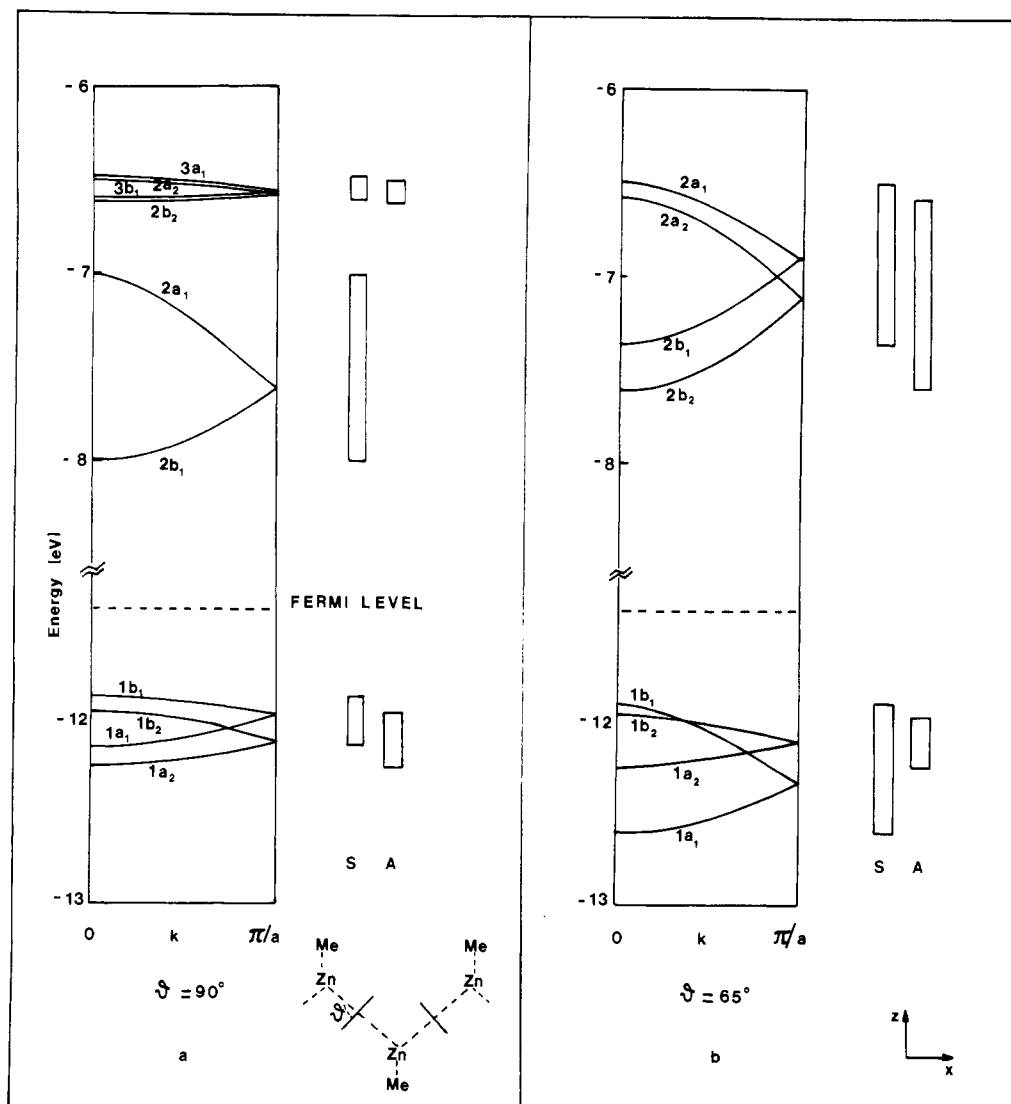


Figure 3. One-dimensional band structure for the $(\text{CH}_3\text{ZnCp})_n$ chain at $\theta = 90^\circ$ (a) and at $\theta = 65^\circ$ (b).

is 2.165 Å).¹² This is indicative that Cp–Mn antibonding orbitals are occupied as would be expected for the high-spin case. The average Mn–C distance in $(\text{Cp}_2\text{Mn})_n$ is very similar to the values in the monomeric high-spin $(\text{MeCp})_2\text{Mn}$ (2.433 Å^{13a}) and Cp_2Mn (2.383 Å¹⁴) but larger than the corresponding value in the low-spin $(\text{MeCp})_2\text{Mn}$ (2.144 Å^{13a}) or $(\text{Me}_5\text{Cp})_2\text{Mn}$ (2.114 Å^{13b}). By drawing an analogy between the high-spin d^5 case and the d^{10} Zn(II) case already treated, we might have expected the similar structural behavior observed. Our attempts to verify this speculation through detailed calculations were only marginally successful. When the d bands obtained in these calculations were assumed to be singly occupied (a magnetic insulating ground state) throughout the Cp tilting distortion, only a weak preference for the tilted geometry was found. Despite the limitations to the extended Hückel method in treating high-spin systems, we feel the reasoning outlined above to be essentially correct but better quality calculations are required to solve the theoretical challenge posed by this system.

Extrapolation to New Polymers. We have seen in what way the structure of the above polymers depends on the number of electrons at the metal center. Polymers are also very sen-

Table I

		ζ		C_1	C_2
Mn ¹⁷	4s	-9.75	1.8		
	4p	-5.89	1.8		
	3d	-11.67	5.15	1.9	0.5311 0.6479
Zn ¹⁸	4s	-12.41	2.01		
	4p	-6.53	1.70		
Pb	6s	-15.7	2.35		
	6p	-8.0	2.06		

sitive to steric factors. For instance, while manganocene polymerizes, permethylmanganocene is a monomer in the solid state. We therefore present the following suggestions for new polymers.

(1) Cp_2Sn does not polymerize in the solid state, probably due to the steric hindrance at the Sn. We have seen that a cyclopentadienyl can be replaced by a methyl group without altering the bonding properties of the main-group element (this isolobal analogy does not apply to a transition-metal atom). It may thus be possible to polymerize CH_3SnCp . In such a polymer, the bridging cyclopentadienyl should be perpendicular to the Sn–Sn direction.

(2) The replacement of Pb by Zn resulted in the removal of four electrons per unit cell. An analogous electron count change is achieved by keeping the metal and replacing a cyclopentadienyl by borole. Thus the bridging borole group

(12) Berndt, A. F.; Marsch, R. E. *Acta Crystallogr.* **1963**, *16*, 118.

(13) (a) Almennigen, A.; Haaland, A.; Samdal, S. *J. Organomet. Chem.* **1978**, *149*, 219. (b) Freyberg, D. P.; Robbins, J. L.; Raymond, K. N.; Smart, J. C. *J. Am. Chem. Soc.* **1979**, *101*, 892.

(14) Haaland, A. *Inorg. Nucl. Chem. Lett.* **1979**, *15*, 267.

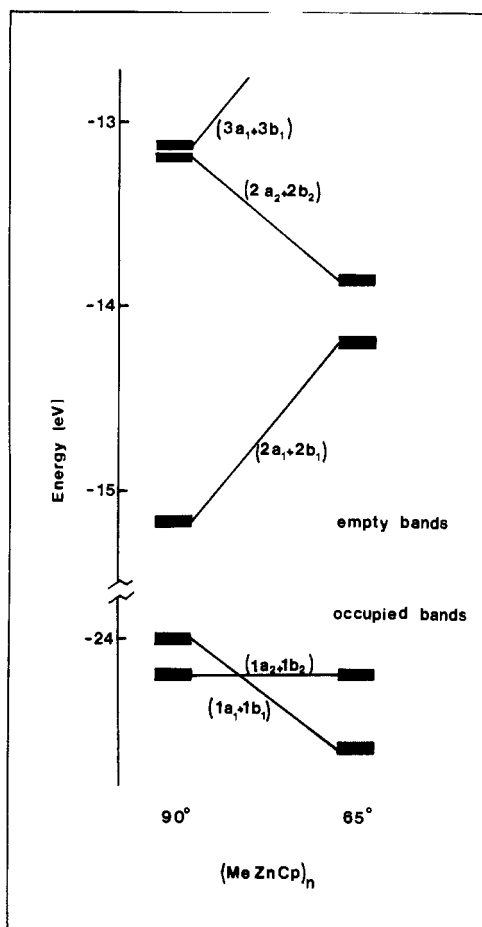


Figure 4. Solid-state Walsh diagram for the variation of θ from 90 to 65° in $(\text{CH}_3\text{ZnCp})_n$.

in $(\text{BC}_4\text{H}_5)_2\text{Pb}$ should be inclined with respect to the Pb-Pb direction.

(3) More bands could be emptied by a systematic replacement of carbon by boron in the cyclopentadienyl ligands.

Boron heterocycles are currently employed as bridging ligands in triple-decker or higher order systems.¹⁵ Interesting electronic and magnetic properties may be expected. The electron count can be further tuned by changing the nature of the main-group metal center. An ample range of interesting polymeric systems can be envisaged on this basis.

Acknowledgment. We are grateful to Dr. S. D. Wijeysekera for his help in adapting the band program and to Professor T. A. Albright for communication of results prior to publication. E.C. thanks the Department of Chemistry of the University of Michigan for their hospitality. O.E. acknowledges the donors of the Petroleum Research Fund, administered by the American Chemical Society, for support of this research.

Appendix

The exponents and parameters are given in Table I. The modified weighted Wolfsberg-Helmholtz formula was used.¹⁶ The following structural parameters were used: Pb-center capping Cp = 2.486 Å, Pb-center bridging Cp = 2.818 Å, C-C(Cp) = 1.4095 Å, C(Cp)-H = 1.08 Å; Zn-C(CH₃) = 1.97 Å, C(CH₃)-H = 1.09 Å, Zn-center bridging Cp = 2.455 Å; Mn-center capping Cp = 2.095 Å; Mn-center bridging Cp = 2.69 Å; $\angle\text{Pb-Pb-Pb} = 120^\circ$, $\angle\text{Zn-Zn-Zn} = 148^\circ$, $\angle\text{Mn-Mn-Mn} = 120^\circ$.

Registry No. $(\text{Cp}_2\text{Pb})_n$, 90623-40-8; $(\text{CH}_3\text{ZnCp})_n$, 90623-41-9; $(\text{Cp}_2\text{Mn})_n$, 90623-42-0.

- (15) Siebert, W. *Adv. Organomet. Chem.* **1980**, *18*, 301.
- (16) Ammeter, J. H.; Bürgi, H.-B.; Thibault, J. C.; Hoffmann, R. *J. Am. Chem. Soc.* **1978**, *100*, 3686.
- (17) Summerville, R. H.; Hoffmann, R. *J. Am. Chem. Soc.* **1976**, *98*, 7240.
- (18) Silvestre, J.; Albright, T. A. *Isr. J. Chem.* **1983**, *23*, 139.
- (19) In fact, a minimum in the total energy is found for θ near 90°. If θ takes on larger values, the structure is destabilized by loss of bonding interactions in lower bands.

Contribution from the Department of Chemistry, Faculty of Science, Kyushu University, Higashiku, Fukuoka 812, Japan

Examples of Fast and Slow Electronic Relaxation between ⁶A and ²T

YONEZO MAEDA,* NAOTO TSUTSUMI, and YOSHIMASA TAKASHIMA

Received April 15, 1983

The iron(III) complexes $[\text{Fe}(\text{sapa})_2]\text{Y}^{3/2}\cdot\text{H}_2\text{O}$, $[\text{Fe}(\text{vapa})_2]\text{Y}$, $[\text{Fe}(\text{acpa})_2]\text{Y}\cdot\text{H}_2\text{O}$, and $[\text{Fe}(\text{bzpa})_2]\text{Y}\cdot 2\text{H}_2\text{O}$ ($\text{Y} = \text{PF}_6$, BPh_4 , NO_3) were synthesized, and the phenomenon of the spin transition between the low-spin ($S = 1/2$) and high-spin ($S = 5/2$) states depending on temperature was confirmed by the temperature-dependent magnetism and Mössbauer spectra. The tridentate ligands used here were *N*-salicylidene-2-pyridylmethylamine (Hsapa), *N*-(3-methoxysalicylidene)-2-pyridylmethylamine (Hvapa), *N*-(1-acetyl-2-propylidene)-2-pyridylmethylamine (Hacpa), and *N*-(1-benzoyl-2-propylidene)-2-pyridylmethylamine (Hbzpa). The "time-averaged" Mössbauer spectra between the low- and high-spin states were observed for $[\text{Fe}(\text{acpa})_2]\text{BPh}_4\cdot\text{H}_2\text{O}$, $[\text{Fe}(\text{bzpa})_2]\text{PF}_6\cdot 2\text{H}_2\text{O}$, and $[\text{Fe}(\text{acpa})_2]\text{NO}_3\cdot\text{H}_2\text{O}$; the relaxation time of the change from the high-spin to the low-spin state (and vice versa) is faster than the ⁵⁷Fe Mössbauer lifetime (1×10^{-7} s). The activation energy for the spin-interchange crossing was calculated to be 2.4 kcal/mol for solid $[\text{Fe}(\text{acpa})_2]\text{BPh}_4\cdot\text{H}_2\text{O}$. The results are interpreted in terms of a model in which the spin-interchange crossing is treated as an intramolecular mechanism, internal electron-transfer reaction. The ground-state Kramers doublet in the $[\text{Fe}(\text{acpa})_2]^+$ series has one unpaired electron in a d_{xy} orbital.

Introduction

Transition-metal complexes exhibiting "spin crossover" between thermally populated low- and high-spin states have been recognized since Cambi et al. first observed "magnetic isomerism" for the tris(dithiocarbamato)iron(III) complexes

in 1931.¹ Since then, a number of spin-crossover complexes of Fe(III),²⁻⁴ Fe(II),^{5,6} and Co(III),⁷ etc., have been studied.

- (1) L. Cambi, L. Szego, and A. Cagnasso, *Atti Accad. Naz. Lincei, Cl. Sci. Fis., Mat. Nat. Rend.*, **15**, 266 (1932).